Penerbit Akademia Baru

Journal of Advanced Research in Materials Science
ISSN (online): 2289-7992 | Vol. 22, No.1. Pages 11-27, 2016

Numerical Study on Turbulent-Forced Convective Heat Transfer of Ag/Heg Water Nanofluid in Pipe

G. Y. Ny[*,1], *N. H. Barom*[a], *S. M. Noraziman*[b] *and S. T. Yeow*[c]

[1]Department of Polymer Engineering, Faculty of Chemical Engineering Universiti Teknologi Malaysia, 81310 Skudai Johor, Malaysia.
[2]Department of Thermofluid, Faculty of Mechanical Engineering Universiti Teknologi Malaysia, 81310 Skudai Johor, Malaysia.
[*]*goyenny0130@gmail.com*, [a]*haziqahbarom@gmail.com*, [b]*sitimasyitanoraziman@gmail.com*, [c]*siewtienyeow@yahoo.com*

Abstract – *Nanofluids is the mixing of nano sized particles with a base fluid. In Recent study, nanofluid of Ag/ Heg gains the interest of some researchers, however, the heat transfer enhancement viability of the Ag/ Heg is controversial. The present study involved the numerical study (Ansys Fluent) of forced convective heat transfer in turbulent pipe flow of silver/ graphene (Ag/ Heg) nanofluid in a stainless steel straight circular pipe with the geometry of 0.01m in hydraulic diameter and 0.8m length with the aim to investigate the heat transfer enhancement of the Ag/ Heg water under different low concentration of volume fraction of Ag/ Heg nanofluid consisting of 0.1%, 0.2%, 0.3%, 0.5%, 0.7% and 0.9%. The pipe flow that subjected to a constant heat flux of 1000W/m^2 are tested under Reynold number of 100000 and 120000. Nanoparticles increase the heat transfer rate by increasing the thermal conductivity of the base fluid. In the current work, the results demonstrate the heat transfer enhancement through Ag/ Heg via realizeable k-ε turbulence model as Nusselt number increases with the increasing Reynold number and a reduction of the nanofluid velocity is detected at the end towards the axial direction. Maximum heat transfer of Ag/ Heg happen at 0.1% volume concentration with the increment of Nusselt number approximately 17.97% by raising the Reynold number from 100000 to200000. The finding obtained are found to have a good agreement with the theoretical and mathematical work in open literature.*

Keywords: Ag/ Heg Water Nanofluids, Turbulent-convective Heat Transfer, Circular Pipe, Reynold Number

1.0 INTRODUCTION

In past decades, different techniques have been brought out in order to enhance the heat transfer rate or increase the efficiency of traditional heat exchangers in various engineering applications, such as: radiators in motor vehicles [1], micro channel in micromachining technology [2], cooling down electronics part or any refrigeration system. These techniques proposed by early scientists can be categorised into two group, namely active technique and passive technique [3]. Usually, active techniques would require the use of power supply and can involve mechanical parts whereas the passive techniques are independent of external sources. Thus, passive techniques have been widely explored as it can lower the existing system operating costs yet possessing high reliability [3].

Journal of Advanced Research in Materials Science
ISSN (online): 2289-7992 | Vol. 22, No.1. Pages 11-27, 2016

The introduction of fins, well-engineered surface texturing [4] and micro channels are among the passive techniques that were widely used. Besides that, the application of novel coolants with enhanced thermo physical properties had also attract attentions as they seem to be the replacement for the conventional heat transfer fluid that possess low thermal conductivity such as water, oil, ethylene glycol, etc [1]. In fact, there were records that scientist had been trying to incorporate high thermal conductivity millimetre and micrometre scaled particles in conventional coolants to create a blend with enhanced thermal properties. Yet, this approach was less convincing as it also associated with high pressure drop, clogging of flow and even corrodes the components in heat exchanger system.

Nevertheless, this idea had been brought out again lately with the advancement of the powder manufacturing techniques that result in synthesising nanosized particles [5]. Nano-fluids are engineered colloidal suspensions prepared by dispersing solid nanosized particles (10 – 100nm) in a base fluid to enhance transport properties. The introduction of solid nanoparticles can also improve the thermal characteristics of the base fluid [6]. Besides being a novel coolant for heat exchanger, nanofluids have the potential to reduce the dimensions of traditional heat exchangers and can also act as magnetic sealants, lubricants [7], and had showed great potential in biomedical sector for antibacterial applications [8].

Nanofluids TiO_2–water suspensions were reported to have up to 30% increment in thermal conductivity when compared to base fluid such as water, ethylene glycol, engine oil and ethanol when the small amount of TiO_2 nanoparticles were distributed uniformly and stably into the suspensions [9]. The small amount nanoparticles had altered the thermophysical properties, affecting overall heat transfer efficiency, thermal conductivity, specific heat capacity, density and also viscosity of the fluid suspensions [10]. Yet, increment in viscosity and corrosion rate of mechanical components are drawbacks of utilizing nanofluids [1].

Nanofluids' thermo physical properties are highly dependence on characteristics of host fluid (water, ethylene glycol, engine oil or mixture of them) [11]. In addition, to obtain a stable suspension of nanofluids, desired coatings and stabilizers have to be deployed according to the hydrophilic or hydrophobic properties of both nanofluids and host fluid [12].

The typical materials for nanoparticles core can be classified into ceramic based such as ceramic based core (CuO, Al_2O_3, TiO_2, SiC, SiO_2, Fe_3O_4, ZnO); metallic based core (Cu, Al, Ag, Au, Fe) or carbon- based core (carbon nanotube, graphene) [13]. While the coatings of the nanoparticles can be molecular or polymeric composition [14]. In Yeul Jung findings, he used ceramic based nanoparticles (Al_2O_3 particles) of diameter 170 nm at the volume fractions of 0.6%, 1.2% and 1.8% and astonishingly, the addition of 1.8% volume fraction of ceramic based nanoparticles into the base fluid had as increment of 32% in heat transfer coefficient when compared to distilled water in laminar region. There is also an increment in the Nusselt numbers with the increment of Reynold numbers [15]. While the other experiment conducted by Lee and Mudawar shows that the heat transfer coefficient increases for single-phase Al_2O_3-water nanofluid suspensions due to high thermal conducticity of nanfluids however the enhancement is not so noticeable in developed region due to the development of thermal boundary layer. While two-phase nanofluids end up as catastrophic failure when applied in a microchannel [16].

In Maxwell's studies, he pointed that thermal conductivity of fluids can be enhanced by incorporating high thermal conductivity [17]. Metallic based core nanoparticle is known to possess high thermal conductivity as metal solid particles have small inter atomic space which

Journal of Advanced Research in Materials Science
ISSN (online): 2289-7992 | Vol. 22, No.1. Pages 11-27, 2016

ease the thermal conduction. In Chein and Chuang study, the experimental results had showed that CuO-H2O nanofluid suspension can absorb more heat and attained lower wall temperature when compare to pure liquid even when the volume fraction of CuO in H2O is as low as 0.2% and 0.4%. Yet, the enhancement of thermophysical properties had also accompanied with slight increase in pressure drop [18].

Carbon based nanoparticles is the most widely used materials due to its high thermal conductivity, high electrical conductivity, high mechanical strength, have great charge carrier's mobility, extremely large surface area and etc [19]. Besides its excellent mechanical properties, carbon based nanoparticles such as graphene is easy and to synthesize and the cost of synthesising is cheaper when compared to nanoparticles with different materials. However, researchers had observed that properties of graphene can have slight variation due to method of synthesising and it is affected by the quantity of graphene sheet in the nanoparticle. The method of synthesising graphene are micromechanical cleavage, chemical vapour deposition, exfoliation of graphite oxide and etc [20].

However, study had shown that dispersing composite nanoparticles into base fluid will yield better heat transfer performance fluid (hybrid nanofluid) when compared to nanofluid that contain single nanoparticle [17]. Few papers had pointed out that nano-fluid consisting silver nano-particles have good thermal conductivity [17]. However, a better thermal conductivity was spotted by Jha and Ramaprabhu [21] when the multi-walled carbon nanotubes were coated by silver nano-particles. Although a number of numerical on the nanofluid of Ag/ Heg on its heat transfer enhancement under the forced convective condition in a turbulent pipe flow, the result still is ambiguous and being debated of it heat transfer ability across Reynold number and different concentration on volume fraction. The effect of volume fraction and Reynold number under the constant heat flux condition by evaluating the impact of axial heat energy transfer in the substrate on the local and average Nusselt number in the length of the pipe are insufficient available to determine the hydro-dynamically and thermally developing flow along the length. Circular pipes are most of the concern of the study of fluid in heat exchangers, piping tube in oil and gas, air conditioning system, biological sensor equipment and so on..

To this purpose, this paper aims at running a numerical study on turbulent-forced convective heat transfer of Ag/ Heg-water nanofluid in pipe as most flows in engineering application such as heat exchanger are turbulence flow and the study of forced convective heat transfer within the hybrid nanofluid with pipe can simulate almost all heat exchanger application that use air as heat sink. In this report, Ag/Heg-water (silver/graphene-water hybrid nanofluid) was used as it is so far, the hybrid nanofluids that better thermal conductivity that had been verified experimentally.

2.0 METHODOLOGY

2.1 Physical Model

The model of the problem has been set as a 3D circular pipe with 0.01m diameter and 0.8m length as shown in Figure 1. The wall was applied with a constant heat flux at 1000 W/m^2 with an inlet temperature set as 293K. The hybrid nanofluid that consisted of silver/graphene Ag/Heg water particle was used. Different volume fractions were tested at Reynold number of 100,000 and 120,000 which indicates a turbulence flow model. Assuming no slip wall at the

Penerbit Akademia Baru

Journal of Advanced Research in Materials Science
ISSN (online): 2289-7992 | Vol. 22, No.1. Pages 11-27, 2016

wall of the pipe, the velocity of the fluid layer at the wall is zero. The simulation was done with few assumptions [2] as the following:

i. The flow was forced convection turbulence flow
ii. Steady state and single phase
iii. Incompressible flow
iv. Fully developed flow
v. No slip wall in hydraulic boundary condition
vi. The flow is axis-symetrical.

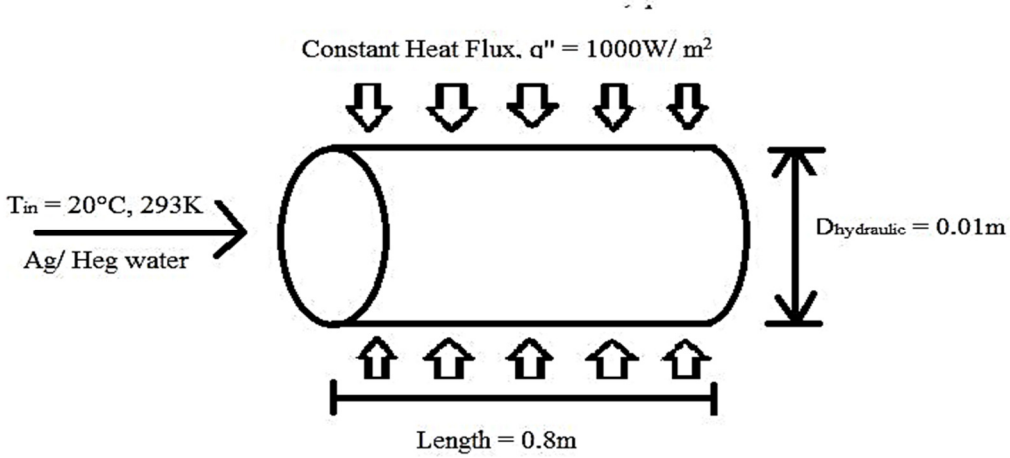

Figure 1: Geometry of circular pipe

Table 1: Properties of Ag/Heg nanofluif at given volume fraction

Volume Fraction	0.1	0.2	0.3	0.5	0.7	0.9
density	1003.581	1008.963	1014.345	1025.109	1035.873	1046.636
Cp	4156.65	4134.201	4111.752	4066.854	4022.423	3969.545
Thermal conductivity,k	0.600608	0.601201	0.601795	0.602982	0.604166	0.605346
μ	0.001006	0.001008	0.001011	0.001016	0.001021	0.001026
Velocity for Re=100k (m/s)	10.0241	9.9905	9.967	9.9111	9.8564	9.8028
Velocity for Re=120k	12.0289	11.9885	11.9604	11.8934	11.8277	11.7634
Prandtl number, Pr	6.962261	6.931583	6.9076368	6.849116	6.794295	6.727981

2.2 Mathematical Formulation

Continuity, momentum and energy equations in 3D are used for incompressible fluid. The governing equations are presented [22] as the following;

Continuity equation:

$$\frac{\delta}{\delta x}(\rho u_i) = 0 \quad (1)$$

Momentum equation:

$$\frac{\delta}{\delta x_i}(\rho u_i u_j) = \frac{\delta \rho}{\delta x_i} + \frac{\delta}{\delta x_i}\left[(\mu + \mu_i)\frac{\delta}{\delta x_i}\right] + \frac{\delta}{\delta x_i}\left[(\mu + \mu_i)\frac{\delta}{\delta x_j}\right] \quad (2)$$

Energy equation:

Penerbit Akademia Baru
Journal of Advanced Research in Materials Science
ISSN (online): 2289-7992 | Vol. 22, No.1. Pages 11-27, 2016

$$\frac{\delta}{\delta x_j}(\rho u_j T) = \frac{\delta}{\delta x_j}\left[\left(\frac{l}{C_p} + \frac{\mu_i}{\sigma_i}\right)\frac{\delta T}{\delta x_j}\right] \quad (3)$$

In addition of application of k – ε turbulence model, the standard k – ε turbulence model has two transport equations of turbulent kinetic energy and rate of dissipation were defined [2];

$$\frac{\delta}{\delta t}(\rho k) + \frac{\delta}{\delta x}(\rho k u) = \frac{\delta}{\delta x}\left[\left(\mu + \frac{\mu}{\sigma}\right)\frac{\delta k}{\delta x}\right] + G + \rho\varepsilon \quad (4)$$

$$\frac{\delta}{\delta t}(\rho\varepsilon) + \frac{\delta}{\delta x}(\rho\varepsilon u) = \frac{\delta}{\delta x}\left[\left(\mu + \frac{\mu}{\sigma}\right)\frac{\delta\varepsilon}{\delta x}\right] + C_1\frac{\varepsilon}{k}(G) - C_2\rho\frac{\varepsilon^2}{k} \quad (5)$$

By applying the first law of thermodynamics, the energy balanced equation [23] become;

$$Q_C = mCp(T_1 - T_2) \quad (6)$$

where, Q_C represents the thermal power exchanged by convection. $T_1 \& T_2$ represents the centreline temperature of inlet and outlet, m is the mass flow rate and Cp is a specific heat. According to G. Ibrahim, [24] the total heat transferred by forced convection is equal to the rate at which thermal energy of the fluid rises. Hence, applying the Newton's Law of Convection that is

$$Q_C = hA\Delta T \quad (7)$$

A = inner surface area of cylindrical pipe, (m^2)
h = convective heat transfer coefficient, ($W/m^2.K$)
ΔT = average wall temperature difference, (K)

Hence, convective heat transfer coefficient at known operating conditions obtained as following;

$$h = \frac{Q_C}{A\Delta T} \quad (8)$$

The surface heat flux q''can be written in Q_C term as,

$$q'' = \frac{Q_C}{A} \quad (9)$$

Solve (8) and (9), hence convective heat transfer coefficient is obtained as following;

$$h = \frac{q''}{\Delta T} \quad (10)$$

in where equivalent to

$$h = \frac{q''}{T_s - T_b} \quad (11)$$

T_s is surface temperature while T_B is bulk temperature along the centreline of the geometry. In a case of turbulent model, Dittus – Boelter equation is one of the correlation used to determine overall convective heat transfer coefficient [23]. The equation is

$$Nu = 0.023\mathrm{Re}^{0.8}\mathrm{Pr}^{0.4} \quad (12)$$

Penerbit Akademia Baru
Journal of Advanced Research in Materials Science
ISSN (online): 2289-7992 | Vol. 22, No.1. Pages 11-27, 2016

Where Re is a Reynold number that is

$$\mathrm{Re} = \frac{\rho v D}{\mu} \tag{13}$$

And Pr is Prantl number denote as

$$\mathrm{Pr} = \frac{\mu C_p}{k} \tag{14}$$

Nusselt number also denote as

$$Nu = \frac{hD}{k} \tag{15}$$

For fully develop pipe flow, turbulence intensity at the core is

$$I = 0.16 Re^{-\frac{1}{8}} \tag{16}$$

2.3 Numerical Approach and Validation

2.3.1 CFD Simulation

A numerical steady – state simulation is considered to investigate and solve complex fluid flow and heat transfer model. The simulation was done using the CFD software, FLUENT 16. 2D geometry was used to perform the simulation as the circular channel is considered symmetric, hence shorten the computational time [23,24] as shown in Figure 2. The boundary types are specified as shown in Figure 2 that is inlet is set as velocity inlet, outlet is pressure outlet, centerline is axis and wall is remained as wall.

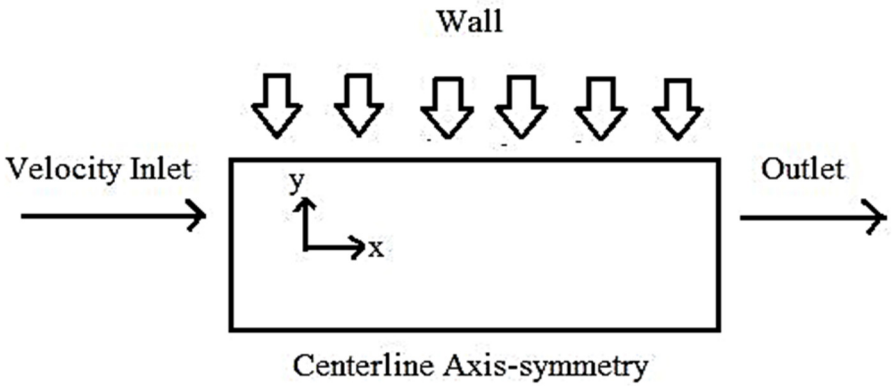

Figure 2: 2D symmetric turbulent pipe flow model

Sizing meshing technique was used in meshing process. There are 80 000 quadrilateral cell in this case used for simulation of 0.1, 0.2, 0.3, 0.5, 0.7 and 0.9 volume fraction of 100K and 120K Reynold number. The Realizable k – ε turbulence model is selected with the near wall enhanced function. The Realizable k – ε turbulence model produces more accurate result at boundary layers flow than a Standard k – ε turbulence model. Additionally, a second – order upwind scheme is adopted in order to discretise momentum, turbulent kinetic energy, turbulent dissipation rate and energy equations. The simulation is modelled with the two dimensional with an Boussinesq approximation to extract the thermal buoyancy effect.

Journal of Advanced Research in Materials Science
ISSN (online): 2289-7992 | Vol. 22, No.1. Pages 11-27, 2016

2.3.2 Grid Independent Test

The 2D computational domain of Ag/Heg nanofluid flows in a turbulent pipe flow is tested under six different mesh sizes that allocate a varieties of cell volume to obtain the optimum mesh size for better accuracy of the data collected. In such circumstances, the grid size consisting of the 10000, 20000, 40000, 80000 and 100000 cell volumes are applied to the grid independent test in the current case. The parameter of the average Nusselt number is used to determine the fluctuation and consistency of the result from the FLUENT numerical simulation. From the Figure 3, increasing pattern of average Nusselt number is observed with the increasing number of cell and remained nearly constant after reaching a peak of the Nusselt number at certain limit of the cell volume which is located at the mesh cell count of 80000 cells. Same pattern of grid independent study is demonstrated by Kumar, 2011 [25]. Increment above the cell count of 80000 lead to insignificant change of the result parameter, yet the simulation is impossible for the cell count of 120000 and above due to the over constrained of the processing equipment of computer. Therefore, in the current simulation, 80000 number of cell is opted for the simulation grid size.

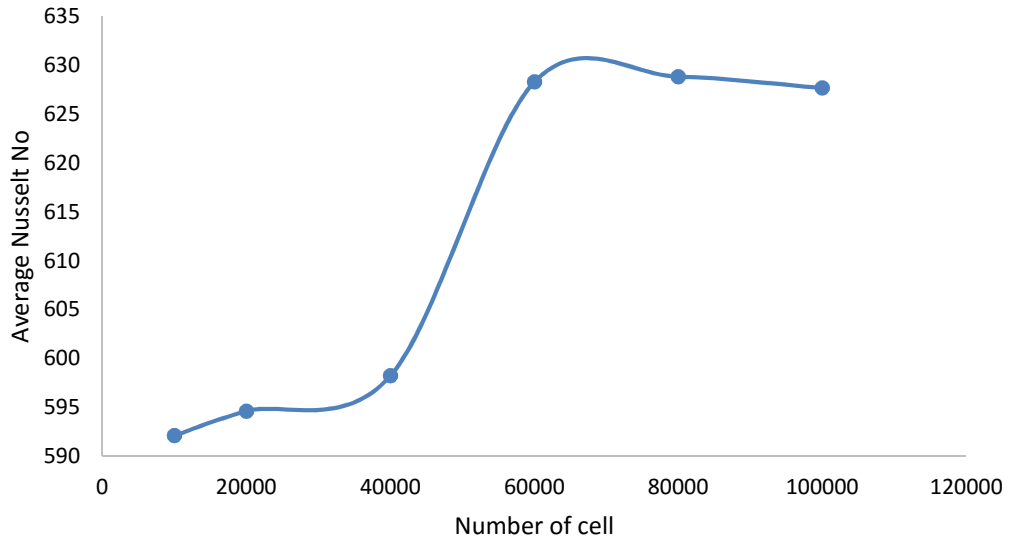

Figure 3: Grid Independence Test

2.3.3 Validation Test

Validation of the model was demonstrated by comparison of the numerical Nusselt number with various turbulence model correlation as shown in both Figure 4 and Figure 5. One of the correlation is the Dittus – Boelter [26] formula as given in Eq. (12) with 0.12% of deviation. The 11% percentage of deviation of Glienlinski correlation [27] is given by

$$Nu = 0.012(Re^{0.87} - 280)\mathrm{Pr}^{0.4} \quad (17)$$

That only true for $3x10^3 \leq \mathrm{Re} \leq 10^6$ and $1.5 \leq \mathrm{Pr} \leq 500$. Another Clienlinski correlation [28] is defined by

Penerbit Akademia Baru
Journal of Advanced Research in Materials Science
ISSN (online): 2289-7992 | Vol. 22, No.1. Pages 11-27, 2016

$$Nu = \frac{\left(f/8\right)(Re-1000)Pr}{1+12.7\left(f/8\right)^{0.5}\left(Pr^{2/3}-1\right)} \quad (18)$$

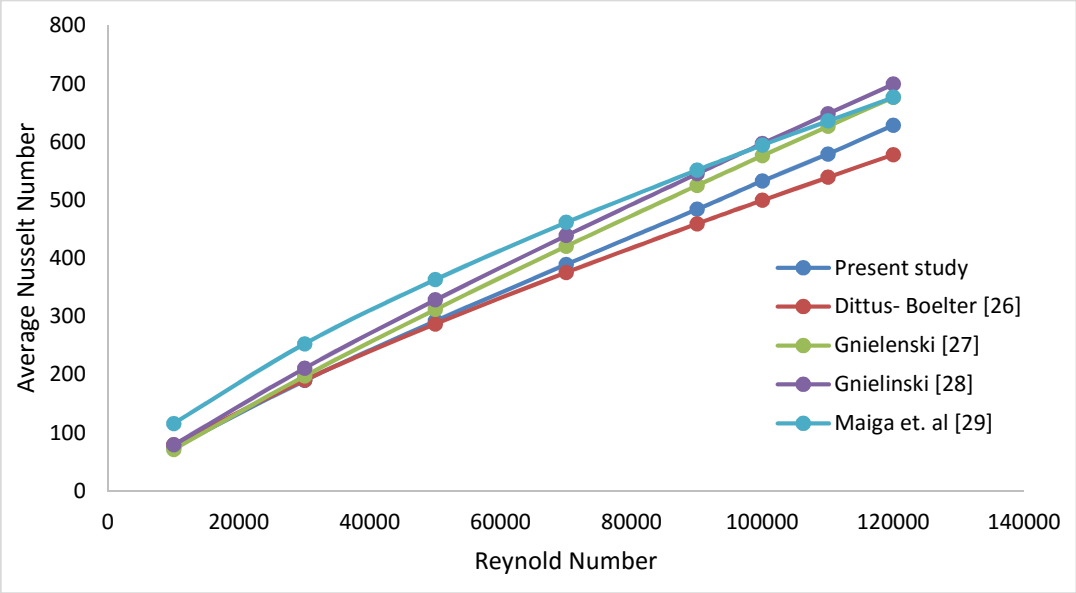

Figure 4: Comparison and Validation of the Present Study in variation of Reynold Number with Other Researchers

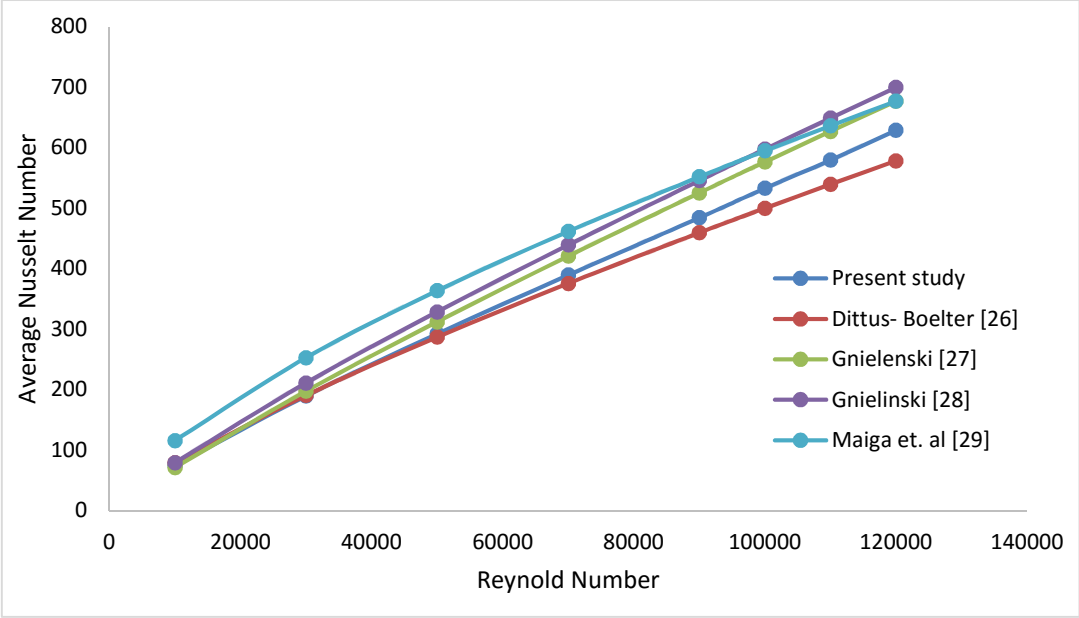

Figure 5: Comparison and Validation of the Present Study in Variation of Volume Fraction with Other Researchers

Where $f = (0.79 \ln \mathrm{Re} - 1.64)^{-2}$ and true for $2300 \leq \mathrm{Re} \leq 10^6$, $0.5 \leq \mathrm{Pr} \leq 2000$. As for many research using the correlation will underestimate the Nusselt number of the nanofluid by considering the Nusselt number for water only, therefore, Miaga correlation [29] presented

Journal of Advanced Research in Materials Science
ISSN (online): 2289-7992 | Vol. 22, No.1. Pages 11-27, 2016

Nusselt number for nanofluid with a 3.3% percentage of deviation is calculated deviated from current research as

$$Nu = 0.085\ \mathrm{Re}^{0.71}\mathrm{Pr}^{0.35} \quad (19)$$

That is only true for for $10^4 \leq \mathrm{Re} \leq 5X10^5$ and $6.6 \leq \mathrm{Pr} \leq 13.9$ as well as volume fraction $0 \leq \phi \leq 10$. The Nusselt number increases with the increases number of Reynold number and decrease with volume fraction in the pipeflow of the Ag/Heg Nanofluid.

3.0 RESULTS AND DISCUSSION

3.1 Effect of Ag/ Heg Volume Concentration On Nusselt Number

Figure 6 represent the change of Nusselt number of 100000 and 120000 Reynolds number for various volume concentration of Ag/Heg nanofluid tested to flow in 0.01m diameter of circular pipe. Obviously observed, the increment of Reynolds numbers had increase the average of Nusselt number of Ag/Heg nanofluid. However, the increasing volume fraction of Ag/Heg nanofluid shows a decrement of the average Nusselt number.

Meanwhile, the effect of Nusselt number on different volume fraction of Ag/Heg nanofluid for 100000 and 120000 Reynolds number of nanoparticles are shown in Figure 7. From an observation, the Nusselt number of Ag/Heg nanofluid decrease with the increasing volume fraction used in the test. For Reynolds number of 100000, the average Nusselt number decrease 1.63% from 0.1% to 0.9% of volume concentration of Ag/He nanofluid while the Nusselt number decrease at 1.67% from the same range of Ag/Heg nanofluid for 120000 Reynolds number.

These result is opposite to the previous researcher on the same study of Ag/Heg nanofluids [6] but in the other hand agreed with Pakravan and Yaghoubi [30] that also indicate the decreasing of Nusselt number with the increasing of volume fraction. Theoretically, different volume fraction of Ag/Heg nanofluid leads to different of its density and dynamic viscosity. With larger nanoparticles in the nanofluid, this will affect the pressure drop and indirectly cause limitation in the application of heat transfer.

From Figure 8, the local Nusselt number for both 100000 and 120000 Reynolds number decrease gradually with the axial distance ratio. However, the average local Nusselt number of 120000 Reynolds number is slightly higher than 100000 Reynold number. In the current case of the nanofluid of Ag/ Heg, the value of the local Nusselt number converge to the value of Nusselt number around 600 for the thermally developed region due to the conjugate effect that causes the distortion of the boundary condition of the solid-fluid interface of Ag/ Heg nanofluids at the beginning of the pipe length. Once the pipe reach the themal develop flow, the heat transfer coeeficient of the pipe flow become nearly constant at axial distance ratio 40. Yet, the conjugation effection of solid-fluid of the nanofluid mixing lead the pipe flow to encounter a “pseudo-isothermal” boundary condition by the convective fluid with excessive conductivity ratio in the axial direction ratio from approximate 5 to before 40, suggesting a low Nusselt number which is the ratio of the convective to conductive heat transfer. This is due to axial back conduction at axial direction 30 to 40 as also observed in Figure 9. In the inlet of the pipe, the local Nusselt number of the pipe is high due to the forced convective.

Penerbit Akademia Baru
Journal of Advanced Research in Materials Science
ISSN (online): 2289-7992 | Vol. 22, No.1. Pages 11-27, 2016

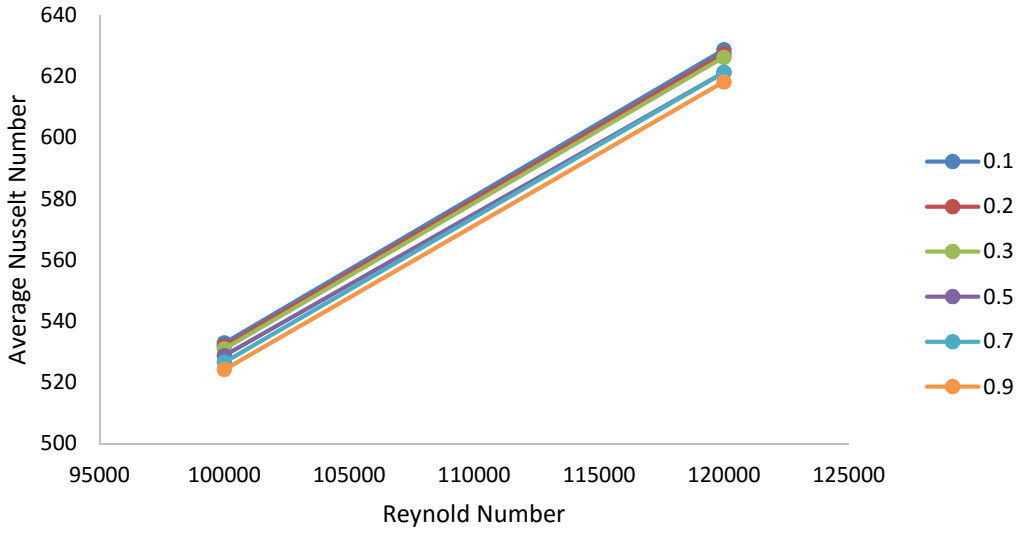

Figure 6: Variation of Average Nusselt Number over Reynold Number with different volume fraction of Ag/ Heg

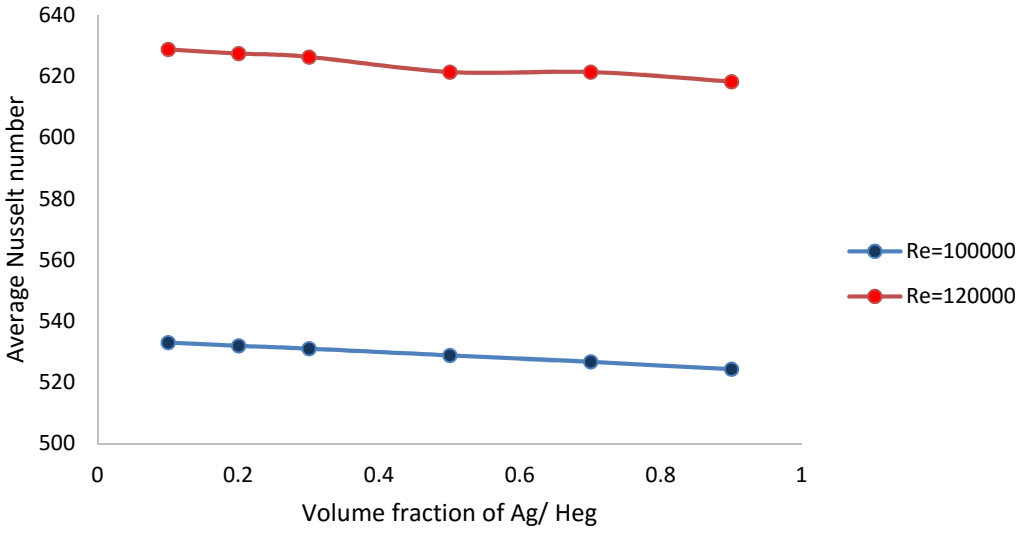

Figure 7: Variation of Average Nusselt Number in different concentration of volume fraction of Ag/ Heg under Reynold Number of 100000 and 120000

Penerbit Akademia Baru
Journal of Advanced Research in Materials Science
ISSN (online): 2289-7992 | Vol. 22, No.1. Pages 11-27, 2016

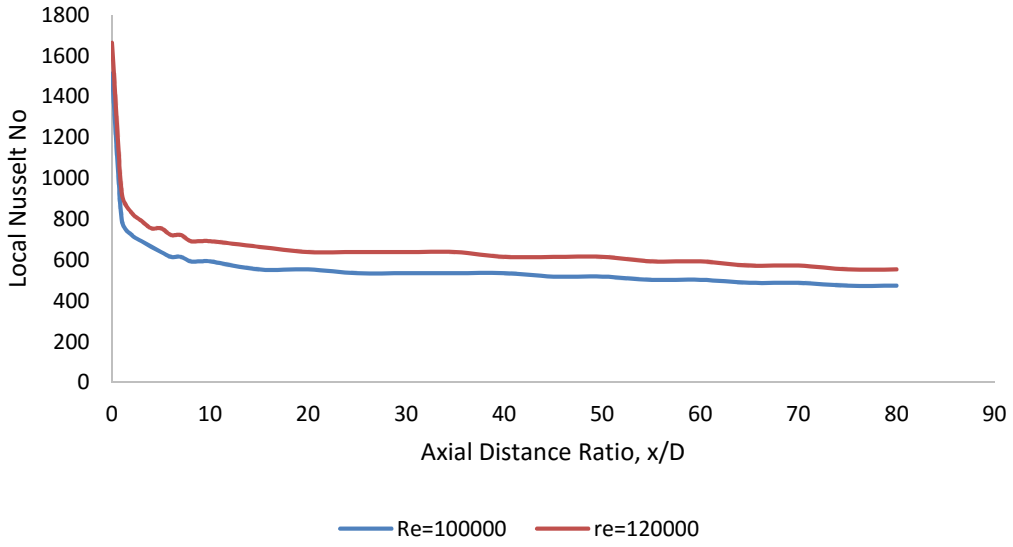

Figure 8: Variation of Local Nusselt Number along the axial distance of the circular pipe in ratio to the diameter of the pipe (x/D)

3.1 Axial and Radial Velocity of Ag/Heg versus distance ratio, x/D

Figure 9 and Figure 10 are the axial velocity of Ag/Heg nanofluid in the circular pipe for 100000 and 120000 Reynolds number correspondingly with variation of volume fractions consisting 0.1%, 0.2%, 0.3%, 0.5%, 0.7% and 0.9% concentration subjected to the axial distance ratio, x/D of the pipe axially. From both graph of 100000 and 120000 Reynolds number, the velocity increase gradually with the distance ratio and reach an optimum axial velocity at approximately 30 distance ratio. The velocity then decreases from approximately 30 to 40 distance ratio and meet a constant velocity from 45 to 80 distance ratio.

Meanwhile Figure 11 represent the radial velocity of Ag/Heg nanofluid in the circular pipe for 100000 and 120000 Reynolds number for a volume fraction of 0.1% concentration subjected to the distance ratio, x/D of the pipe radially. From both lines of 100000 and 120000 Reynolds number, the velocity increase in the same pattern as in axial direction and reaching an optimum velocity at approximately 30 distance ratio and flow at constant velocity at 50 distance ratio.

From all graphs from Figure 9, Figure 10 and Figure 11 it can be stated that the flow of Ag/Heg nanofluid is fully developed in the pipe along the simulation. The velocity is at the lowest value at early distance as it deals with the wall friction factor, however the velocity then reaches a peak value before meet a constant velocity because the turbulence that occur in the pipe, then lastly the velocity is constant nearly at the middle of the pipe indicate that the flow is fully develop.

Penerbit Akademia Baru
Journal of Advanced Research in Materials Science
ISSN (online): 2289-7992 | Vol. 22, No.1. Pages 11-27, 2016

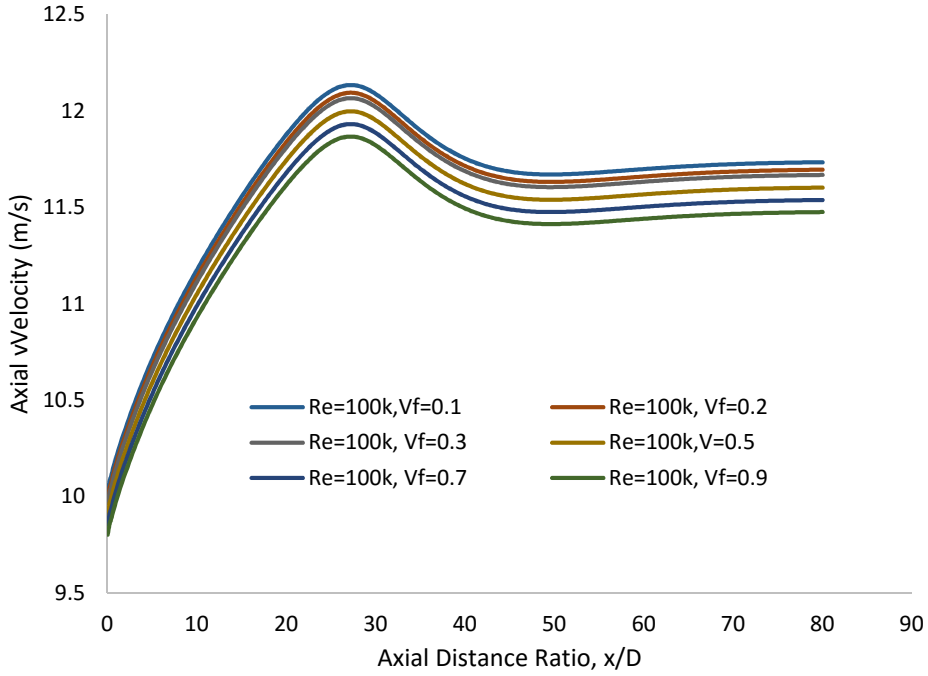

Figure 9: Comparison of axial velocity along the axial distance of the circular pipe in ratio to the diameter of the pipe for Re=100k

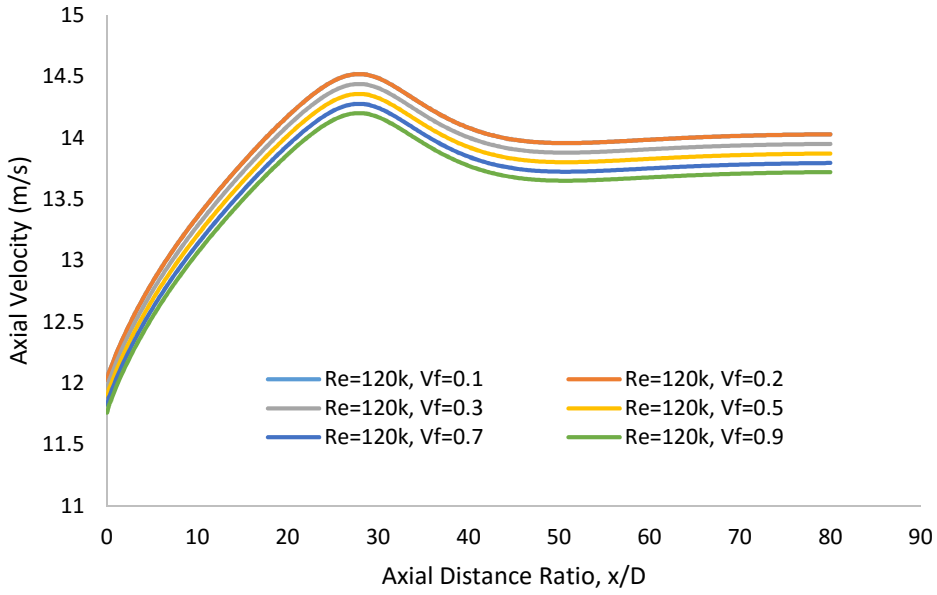

Figure 10: Comparison of axial velocity along the axial distance of the circular pipe in ratio to the diameter of the pipe for Re=120k

Journal of Advanced Research in Materials Science
ISSN (online): 2289-7992 | Vol. 22, No.1. Pages 11-27, 2016

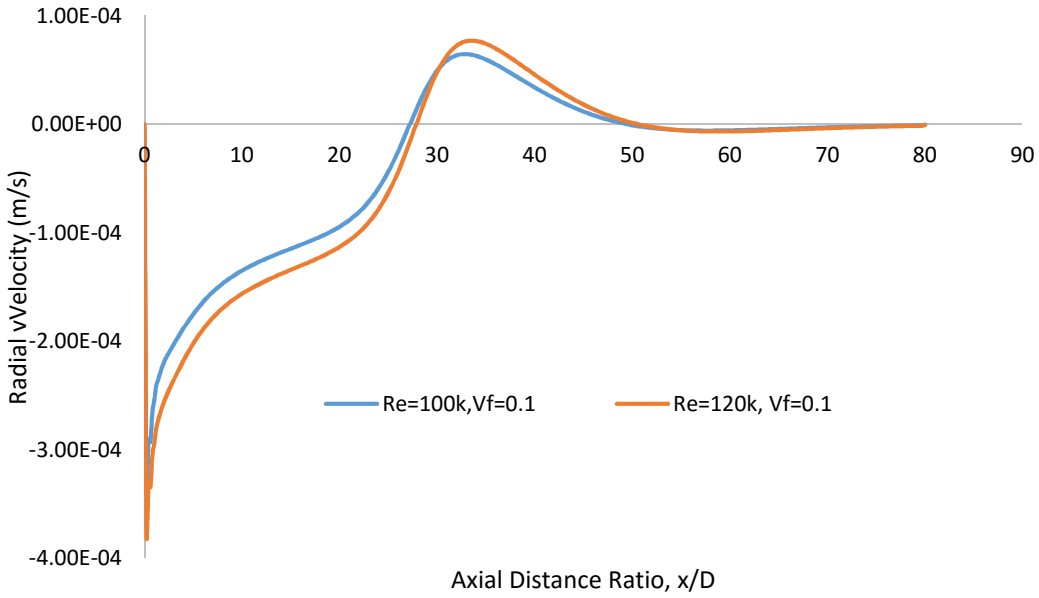

Figure 11: Variation of radial velocity in the axial distance of the circular pipe with the ratio to pipe diameter for two cases of Re (100k and 120k)

4.0 CONCLUSION

This paper presents an inclusive review on the application of nanofluids for cooling of vehicle engine. The vast number of available references shows that nanofluids have a great application prospect in the development of modern engines. For engine cooling system, nanoparticles can be dispersed into the engine oil to enhance the thermal conductivity of the liquid. In addition, the presence of nanoparticles in engine oil will also improve the performance of lubricants and reduce friction. However, the optimum amount of nanoparticles in engine oil still remains unknown.

In this paper, a numerical study has been done using Computational Fluid Dynamic (CFD) software of Ansys Fluent. A few parameters have been carried out such as effect of the Nusselt number on the volume fraction of Ag/Heg nanofluid and the Reynolds number used in the flow of the nanofluids. The velocity profile of axial and radial velocity of the Ag/Heg nanofluid also are observed to ensure the development of flow along the pipe.

From following results, the numerical simulation of Ag/Heg nanofluid, the flow in this study has shown that it can reach a fully developed state in the pipe with the theoretical of near wall function.

In general, it can be concluded that the Nusselt numbers of Ag/Heg nanofuid will increase with the increment of Reynolds number. However, the Nusselt number can have a slightly lower value with the increment of volume fraction of the nanofluid opposed previous researcher. However, it is acceptable as the behavior is due to the dynamic viscosity and the density of the nanofluid itself.

Journal of Advanced Research in Materials Science
ISSN (online): 2289-7992 | Vol. 22, No.1. Pages 11-27, 2016

REFERENCES

[1] Bigdeli, Masoud Bozorg, Matteo Fasano, Annalisa Cardellini, Eliodoro Chiavazzo, and Pietro Asinari. "A review on the heat and mass transfer phenomena in nanofluid coolants with special focus on automotive applications." Renewable and Sustainable Energy Reviews 60 (2016): 1615-1633

[2] Sidik, Nor Azwadi Che, M. M. Yassin, and M. N. Musa. "Turbulent-forced convective heat transfer and pressure drop analysis of Fe3O4 magnetic nanofluid in a circular microchannel." Jurnal Teknologi 75, no. 11 (2015).

[3] Wen, Dongsheng, Guiping Lin, Saeid Vafaei, and Kai Zhang. "Review of nanofluids for heat transfer applications." Particuology 7, no. 2 (2009): 141-150.

[4] Ventola, Luigi, Francesco Robotti, Masoud Dialameh, Flaviana Calignano, Diego Manfredi, Eliodoro Chiavazzo, and Pietro Asinari. "Rough surfaces with enhanced heat transfer for electronics cooling by direct metal laser sintering." International Journal of Heat and Mass Transfer 75 (2014): 58-74.

[5] Choi, Stephen US, and J. A. Eastman. "Enhancing thermal conductivity of fluids with nanoparticles. ASME International Mechanical Engineering Congress & Exposition." American Society of Mechanical Engineers, San Francisco (1995).

[6] Azwadi, CS Nor, and I. M. Adamu. "Turbulent force convective heat transfer of hybrid nano fluid in a circular channel with constant heat flux." J. Adv. Res. Fluid Mech. Therm. Sci 19 (2016): 1-9.

[7] Lee, Kwangho, Yujin Hwang, Seongir Cheong, Laeun Kwon, Sungchoon Kim, and Jaekeun Lee. "Performance evaluation of nano-lubricants of fullerene nanoparticles in refrigeration mineral oil." Current Applied Physics 9, no. 2 (2009): e128-e131.

[8] Zhang, Lingling, Yulong Ding, Malcolm Povey, and David York. "ZnO nanofluids–A potential antibacterial agent." Progress in Natural Science 18, no. 8 (2008): 939-944.

[9] Murshed, S. M. S., K. C. Leong, and C. Yang. "Enhanced thermal conductivity of TiO 2—water based nanofluids." International Journal of thermal sciences 44, no. 4 (2005): 367-373.

[10] Celata, Gian Piero, Francesco D'Annibale, Andrea Mariani, Luca Saraceno, Rosaria D'Amato, and Roberto Bubbico. "Heat transfer in water-based SiC and TiO2 nanofluids." Heat Transfer Engineering 34, no. 13 (2013): 1060-1072.

[11] Timofeeva, Elena V., Wenhua Yu, David M. France, Dileep Singh, and Jules L. Routbort. "Nanofluids for heat transfer: an engineering approach." Nanoscale research letters 6, no. 1 (2011): 1.

[12] Wang, Xiang-Qi, and Arun S. Mujumdar. "A review on nanofluids-part II: experiments and applications." Brazilian Journal of Chemical Engineering 25, no. 4 (2008): 631-648.

[13] Das, S. K., S. U. S. Choi, and W. Yu. "Pradeep, Nanofluids Science and Technology." (2007).

Journal of Advanced Research in Materials Science
ISSN (online): 2289-7992 | Vol. 22, No.1. Pages 11-27, 2016

[14] Krajnik, Peter, F. Pusavec, and Amir Rashid. "Nanofluids: Properties, applications and sustainability aspects in materials processing technologies." In Advances in Sustainable Manufacturing, pp. 107-113. Springer Berlin Heidelberg, 2011.

[15] J-Y. Jung, Oh. Hoo-Suk et al. 2009. Forced convective heat transfer of nanofluids in microchannels. Int. J. of Heat and Mass Transfer 52: 466-472.

[16] J. Lee, I. Mudawar. 2007. Assessment of the effectiveness of nanofluids for single-phase and two-phase heat transfer in micro-channels. Int. J. of Heat and Mass Transfer. 50: 452-463.

[17] Aspnes, David E. "Optical properties of thin films." Thin solid films 89, no. 3 (1982): 249-262.

[18] R. Chein, J. Chuang. 2006. experimental microchannel heat sink performance studies using nanofluids. Int. J. of Thermal Sciences. 46: 57-66.

[19] Novoselov, Kostya S., Andre K. Geim, S. V. Morozov, D. Jiang, Y_ Zhang, SV and Dubonos, I. V. Grigorieva, and A. A. Firsov. "Electric field effect in atomically thin carbon films." Science 306, no. 5696 (2004): 666-669.

[20] Azwadi, CS Nor, and I. M. Adamu. "Turbulent force convective heat transfer of hybrid nano fluid in a circular channel with constant heat flux." J. Adv. Res. Fluid Mech. Therm. Sci 19 (2016): 1-9.

[21] M. Rostamani, S. F. Hosseinizadeh et al. 2010. Numerical study of turbulent forced convection flow of nanofluids in a long horizontal duct considering variable properties, Int. Communications in Heat and Mass Transfer. 37: 1426-1431.

[22] Sadeghinezhad, Emad, Hussein Togun, Mohammad Mehrali, Parvaneh Sadeghi Nejad, Sara Tahan Latibari, Tuqa Abdulrazzaq, S. N. Kazi, and Hendrik Simon Cornelis Metselaar. "An experimental and numerical investigation of heat transfer enhancement for graphene nanoplatelets nanofluids in turbulent flow conditions." International Journal of Heat and Mass Transfer 81 (2015): 41-51.

[23] Abbas, Qaiser, M. Mahabat Khan, Rizwan Sabir, Yasir Mehmood Khan, and Zafar Ullah Koreshi. "Numerical simulation and experimental verification of air flow through a heated pipe." Int. J. Mechanical Mechatronics Eng 10, no. 2 (2010): 7-12.

[24] Ibrahim. G. Hesham. “Experimental and CFD Analysis of Turbulent Flow Heat Transfer in Tubular Exchanger”. International Journal of Engineering and Applied Sciences, no.7 (2014).

[25] Kumar, P. "A CFD study of heat transfer enhancement in pipe flow with Al2O3 nanofluid." World Academy of Science 81 (2011): 746-750.

[26] Dittus, F. W., and L. M. K. Boelter. "University of California publications on engineering." University of California publications in Engineering 2 (1930): 371.

[27] Gnielenski, V. "New equations for heat and mass transfer in turbulent pipe and channels flow." Int. Chemical Engineering 16 (1976): 359-368

Journal of Advanced Research in Materials Science
ISSN (online): 2289-7992 | Vol. 22, No.1. Pages 11-27, 2016

[28] Gnielinski, V., New equations for heat and mass transfer in the turbulent flow in pipes and channels. NASA STI/Recon Technical Report A, 1975. 75: p. 22028

[29] El Bécaye Maïga, Sidi, Cong Tam Nguyen, Nicolas Galanis, Gilles Roy, Thierry Maré, and Mickaël Coqueux. "Heat transfer enhancement in turbulent tube flow using Al2O3 nanoparticle suspension." International Journal of Numerical Methods for Heat & Fluid Flow 16, no. 3 (2006): 275-292

[30] Pakravan, Hossein Ali, and Mahmood Yaghoubi. "Combined thermophoresis, Brownian motion and Dufour effects on natural convection of nanofluids." International Journal of Thermal Sciences 50, no. 3 (2011): 394-402.

Penerbit Akademia Baru

Journal of Advanced Research in Materials Science
ISSN (online): 2289-7992 | Vol. 22, No.1. Pages 11-27, 2016

APPENDIX

Table A: Grid Independent Test tabulated data

No of Cell Count	Average Nusselt Number,
10000	592.1229867
20000	594.6355312
40000	598.2687917
60000	628.3360618
80000	628.8563384
100000	627.7069925

Table B: Tabulated data of numerical approach.

Reynold no/ Nusselt No	Simulation data	Dittus - Boelter	Glienlinski (Dr Azwadi)	Glienlinski	Maiga *et. al*
10k	74.93846662	79.21874465	71.45344232	79.31452988	115.979318
20k		137.9278456	136.6363507	148.0134711	189.7194458
30k	189.8802043	190.7765364	197.5196517	211.0608892	253.009391
40k		240.1463273	255.7687341	270.9031611	310.3438506
50k	292.2806875	287.0806755	312.1342734	328.5898187	363.6212484
60k		332.1612425	367.0428846	384.5864228	413.8738035
70k	389.5768319	375.7564014	420.7687969	439.2626533	461.7428284
80k		418.119041	473.5025716	492.890106	507.6617485
90k	484.3357087	459.4327643	525.3839936	545.6912662	551.9410966
100k	533.059301	499.8364876	576.5197766	597.6111801	594.8131352
110k	579.4625711	539.4387051	626.993927	648.8180828	636.4574243
120k	628.8563384	578.3263135	676.8742081	699.6690183	677.0164717

Table C: Tabulated data of volume fraction numerical validation.

Volume fraction	simulation data	Dittus -Boelter	Glienlinski (Dr Aswadi)	Glienlinski	Maiga et. al
0.1	533.059301	499.8364993	576.5212773	597.6111954	594.81449
0.2	532.0662294	498.9543419	575.5037796	596.4624347	593.8958283
0.3	531.1173813	498.2641411	574.7076884	595.5633002	593.1769248
0.5	528.9335429	496.5713335	572.7551706	593.3567784	591.4131928
0.7	526.8075802	494.9776635	570.9170002	591.2778173	589.7520651
0.9	524.3656079	493.0395347	568.6815242	588.747327	587.7309968

Table D: Properties of SS304 stainless steel

Volume Fraction	SS 304
density	7900
Cp	500
Thermal conductivity,k	15